PROGRESS IN COLOR, COLORANTS AND COATINGS

available online @ www.pccc.icrc.ac.ir

Prog. Color Colorants Coat. 9 (2016), 249-260

Ministry of Science, Research and Technology
Institute for Color Science and Technology

Adsorption and Photocatalytic Properties of Surface-Modified TiO_2 Nanoparticles for Methyl Orange Removal from Aqueous Solutions

A. Mohammadi*, A. Aliakbarzadeh Karimi, H. Fallah Moafi

Department of Chemistry, Faculty of Sciences, University of Guilan, P. O. Box: 41335-1914, Rasht, Iran

ARTICLE INFO

Article history:
Received: 31 July 2016
Final Revised: 12 Sept 2016
Accepted: 14 Sept 2016
Available online: 16 Sept 2016

Keywords:
Methyl Orange
TiO_2 nanoparticles
Surface-modification
5-Sulfosalicylic acid.

ABSTRACT

Surface-modified titanium dioxide nanoparticles by 5-sulfosalicylic acid (5-SA-TiO_2) were prepared in ethanol by the chemisorption process. The effects of surface improvement on the photocatalytic degradation and adsorption of methyl orange (MO) were studied in a batch system by considering various parameters such as contact time, adsorbent dosage, pH, initial dye concentration and temperature. The adsorption and photocatalytic degradation kinetics of MO using the improved nanoparticles have also been investigated. The results show that the adsorption and photocatalytic degradation processes were well fitted with the pseudo-second-order kinetic model (R^2> 0.99). In addition, the equilibrium data for the adsorption process have been evaluated using Langmuir, Freundlich and Temkin isotherms. The adsorption isotherm of MO onto modified TiO_2 nanoparticles fitted into the Temkin equation. Prog. Color Colorants Coat. 9 (2016), 249-260© Institute for Color Science and Technology.

1. Introduction

Azo chromophores are a group of colorant materials characterized by the presence of an azo group (-N=N-) but can contain two, three, or more azo groups. Since their discovery in the 19th century, azo colorants have been widely used in various industries and accounting for over 50% of all commercial dyes [1, 2]. In addition to their use as colorants, azo dyes have been employed for many applications, such as in ink jet printing [3], thermal transfer printing [4], photography [5], color additives [6], biomedical area [7], molecular recognition [8], light controlled polymers [9], liquid crystal industry [10]. Moreover, most of these dyes such as anionic dye methyl orange (MO) are toxic, carcinogenic, and mutagenic [11, 12]. Thus, dye elimination from wastewaters before their discharge into the environment is very essential [13].

In recent years, many procedures such as adsorption, photocatalysis, chemical oxidation, coagulation/flocculation, biological treatment, ozonation, ion exchange, etc. have been developed for separating organic contaminants from water and wastewaters [14-19]. Among the various techniques for removal of organic pollutants, adsorption process has been proven as a highly effective removal method due to its efficiency, simplicity and applicability. In addition, any material that has pores can be used as adsorbent [14, 20]. Several natural and synthetic

*Corresponding author: a-mohammadi@guilan.ac.ir

adsorbents such as activated carbon, chitin, TiO_2, nano-TiO_2, etc. have been used to remove contaminants from wastewaters [21-28]. Among them, nano-TiO_2 have commercial interests for their low cost, photocatalytic activity, large specific surface area, nontoxicity, long service life, high efficiency and simple assemble technology [29, 30]. However, the use of TiO_2 was limited by its polarity, high surface free energy, and poor dispersing capability [31]. Therefore, in order to enhance the photocatalytic activity and adsorption ability, various colorless organic compounds have been used for the surface modification of TiO_2. This surface modification can be done by the interactions between organic coatings and -OH groups on the TiO_2 surface [32]. However, the design and efficient operation of adsorption processes require equilibrium adsorption data. The equilibrium isotherm plays an important role in predictive modeling for analysis and design of adsorption systems [33]. In the present study, surface-modified TiO_2 nanoparticles for the elimination of methyl orange (MO) were synthesized and characterized by means of XRD, SEM, FT-IR. The effects of several parameters such as contact time, photoadsorbent dose, pH, dye concentration and temperature were examined. The photocatalytic and adsorption kinetics, thermodynamics and adsorption isotherms were also studied.

2. Materials and methods

2.1. Chemicals

Methyl orange (MO) was supplied commercially, and used without further purification. The chemical structure of MO is shown in Scheme 1. Titanium isopropoxide (TIP) was obtained from Merck Chemical Company. 5-Sulfosalicylic acid was obtained Commercially and its solutions were used freshly in order to avoid oxidation by dissolved oxygen. All other chemicals were of the highest purity commercially available. De-ionized water was purified with a Milli-Q water ion-exchange system and was used in all experiments.

2.2. TiO_2 nanoparticles preparation and its surface modification with 5-sulfosalicylic acid

TiO_2 nanoparticles were synthesized using the titanium isopropoxide (TIP) according to a method described in the literature [34]. In situ surface modification was carried out through stirring TiO_2 nanoparticles for 60 min in the saturated solution of 5-sulfosalicylic acid. It was worth noting that the color of the TiO_2 changed into yellow, indicating that a chemical reaction takes place (i.e., chemisorption) between 5-sulfosalicylic acid (surface modifier) and TiO_2. After filtration, the modified TiO_2 was washed with water three times and then heat-treated for 30 min at 105 °C. The resulting powders were characterized by XRD, FT-IR and SEM.

2.3. Batch adsorption experiments

To achieve the equilibrium data, the photocatalytic degradation and adsorption of methyl orange from aqueous solutions onto nano 5-SA-TiO_2 was done using batch technique. Methyl orange concentration changes over time with respect to various parameters such as the amount of absorbent, pH, initial dye concentration and temperature were evaluated. The effect of pH on the adsorption of MO was examined by mixing 0.02 g 5-SA-TiO_2 with 25 mL MO solution (20 μM) with the pH values ranging from 3.0 to 10.0. The pH of the samples was adjusted by adding μL quantities of 0.5 M HCl or NaOH. After the photocatalytic degradation and adsorption process, the liquid and solid phases were separated by centrifuging. The UV-Vis spectro-photometer was employed for absorbance measurements of the samples. The maximum wavelength (λ_{max}) used for determination of residual concentration of MO in solution was 460 nm. Morever, the concentrations of MO in the liquor were determined using standard curve. The amount of MO removed was determined by using the following equation:

$$Q_e = \frac{(C_0 - C_e).V}{m} \quad (1)$$

$$\text{Removal } (\%) = \frac{100\,(C_0 - C_e)}{C_0} \quad (2)$$

where Q_e is the adsorption capacity of adsorbent, C_0 and C_e (mg L^{-1}) are concentration of MO at the initial and equilibrium states, respectively, V (L) is the volume of the solution and m is the weight of adsorbent (g).

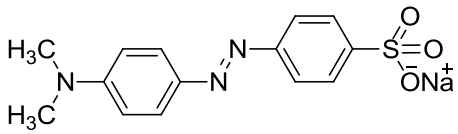

Scheme 1: Molecular structure of Methyl Orang.

3. Results and discussion

3.1.Characterization of samples

The XRD patterns of TiO_2 and 5-SA-TiO_2 ananoparticles are shown in Figure 1. As shown in Figure 1a, characteristic peaks of TiO_2 (2θ = 25°, 38°, 48°, 54°, 55°and 63°) are observed for both pure TiO_2 and surface-modified TiO_2 ananoparticles. These diffraction peaks are attribued to anatase phase. As shown in Figure 1b, the intensity of diffraction peaks in the surface-modified TiO_2 is decreased, which indicates that the surface modification of TiO_2 nanoparticles. This confirms the existence of 5-Sulfosaliccylic acid surface modifier in TiO_2 nanoparticles. The useful groups present in the improved TiO_2 nanoparticles can be evaluated using FT-IR spectroscopy. Figures 2a and 2b show the FT-IR spectra of the pure TiO_2 and 5-SA-TiO_2, respectively. The FT-IR spectra of the 5-SA-TiO_2 nanoparticles show the presence of new absoption peaks (cm^{-1}) such as OH (3406), C=O (1680), C-O (1470), SO_3H (1164 and 1224). These functional groups indicate that the 5-Sulfosaliccylic acid as modifier is chemically immobilized on the surface of nanoparticles. Thus, it can be recognized that the TiO_2 nanoparticles are modified with 5-Sulfosaliccylic acid. In addition, in order to investigate the morphology of the obtained adsorbents, the SEM images of TiO_2 and 5-SA-TiO_2 nanoparticles are illustrated in Figures 3a and 3b. It was found that the surface modifier could not only affect the dispersibility of the modified TiO_2 nanoparticles, but also change their morphology and size. Furthermore, SEM study of TiO_2 and 5-SA-TiO_2 indicate that the particle size of the prepared samples is less than 60 and 65 nm, respectively.

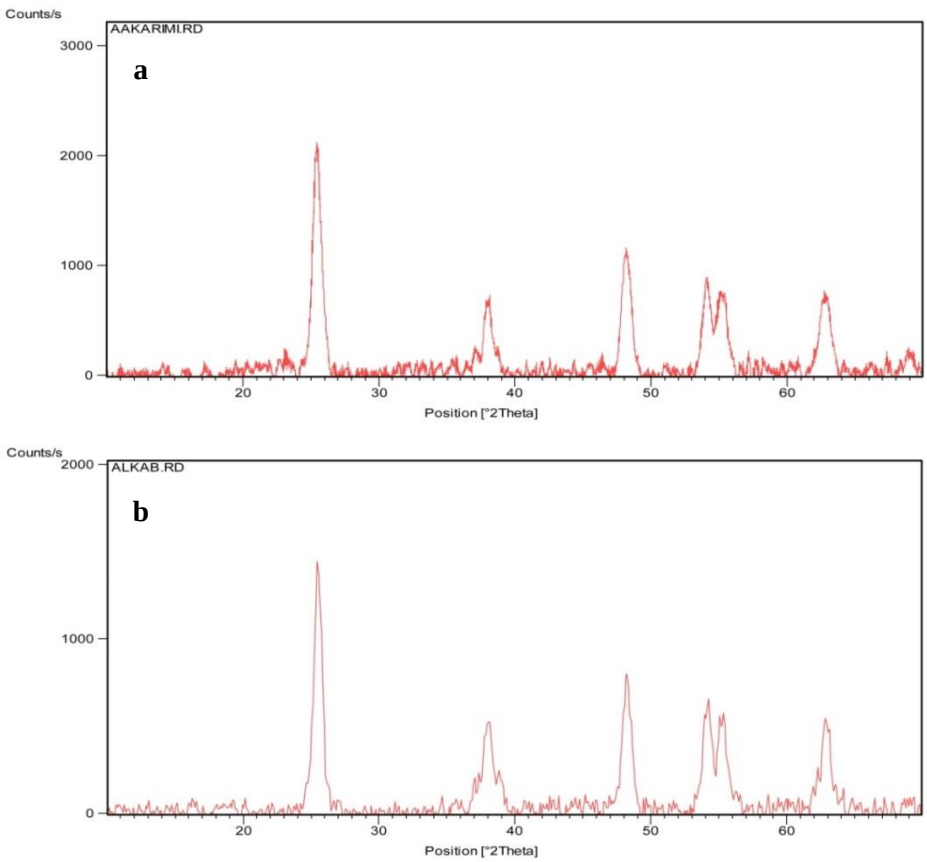

Figure 1: XRD pattern of prepared samples: (a) TiO_2; (b) 5-SA-TiO_2.

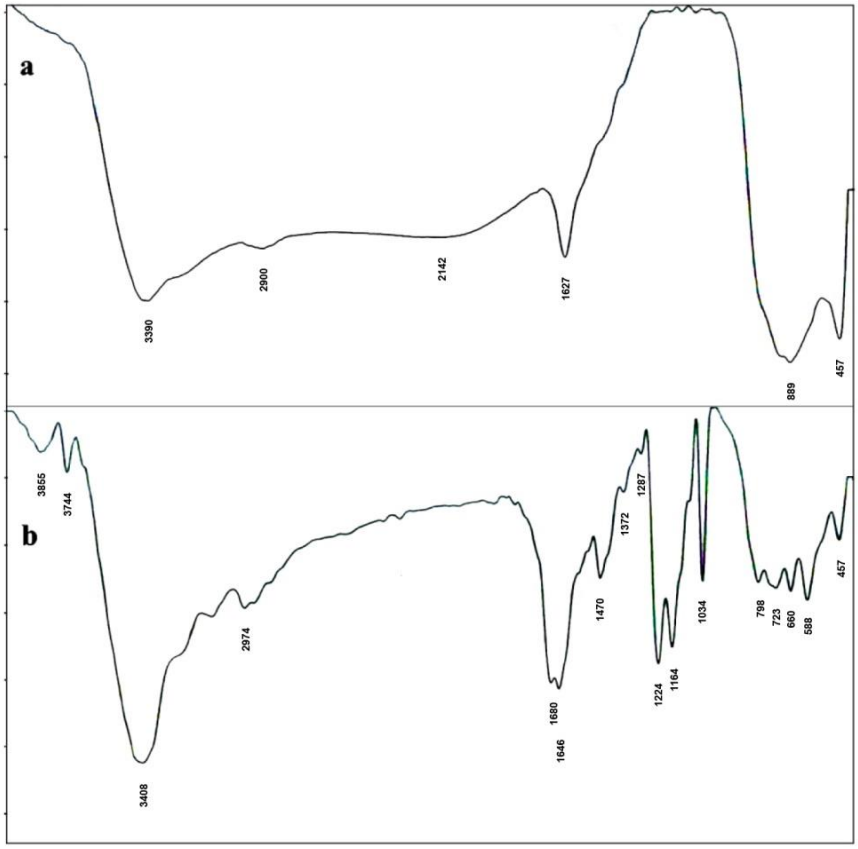

Figure 2: FT-IR spectra of prepared samples: (a) TiO_2; (b) 5-SA-TiO_2.

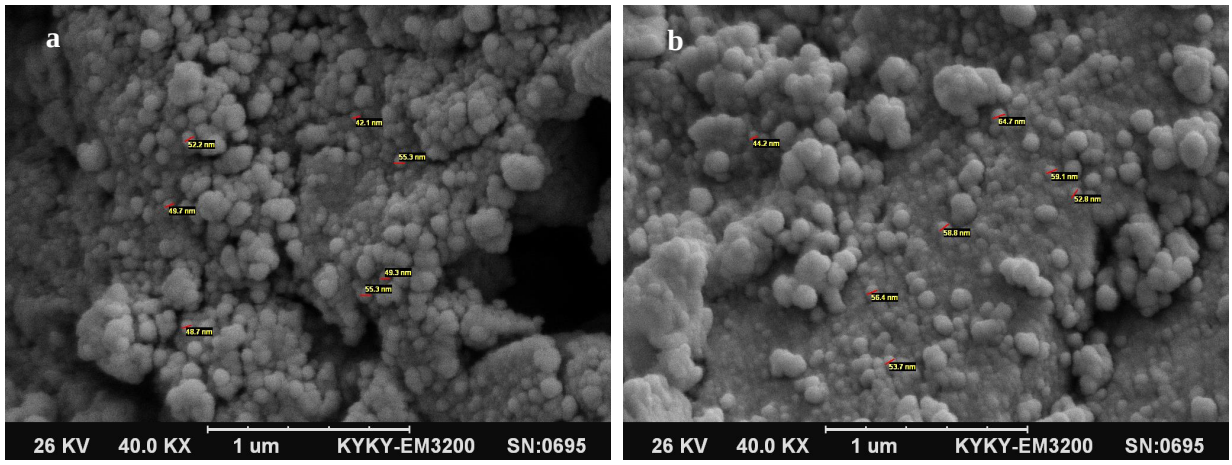

Figure 3: SEM images of prepared samples: (a) TiO_2; (b) 5-SA-TiO_2.

3.2. Effect of pH value on the adsorption and photocatalytic degradation of MO

Figure 4 shows the effect of pH value at a range of 3.00-9.00 on the MO removal onto 5-SA-TiO_2. As shown in Figure 4, the removal capacity increased with increasing pH value from 3.0 to 5.0 and then decreased with the further increase of the pH from 5.0 to 9.0. So, the optimum pH value for the removal of MO was 5.0. The MO acid dye give negatively charged ions (SO_3^-) when dissolved in water. On the other hand, the TiO_2 surface would remain positively charged in acidic medium and negatively charged in alkaline medium. Thus, in acidic medium, positively charged surface of sorbent tends to adsorb anionic species.

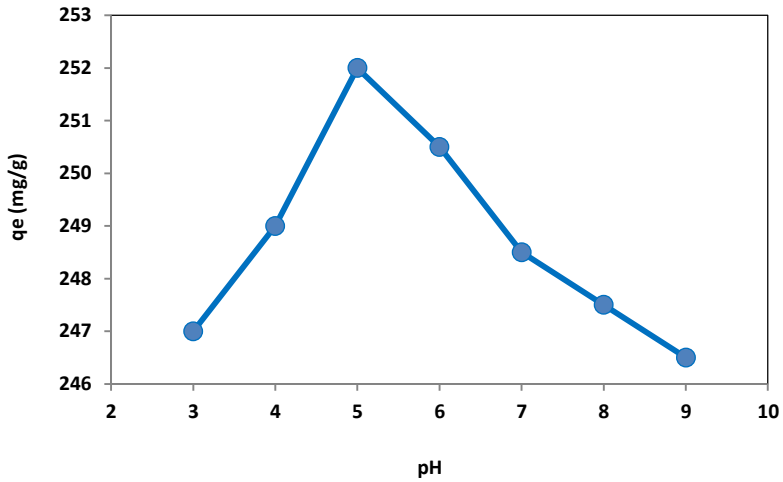

Figure 4: Effect of pH on adsorption of MO (initial concentration 200 mg/L, and T= 298 K).

3.3. Effect of 5-SA-TiO_2 dosage on adsorption and photocatalytic degradation of MO

The effect of catalyst dosage on the adsorption and photocatalytic degradation of MO from aqueous solution is shown in Figure 5, in which the MO removal efficiency increased with the addition of 5-SA-TiO_2 from 0.02 to 0.08 g/L in the adsorption process, because the adsorption surface and accessibility of more adsorption sites increased. However, on the basis of the adsorption capacity in terms of mg adsorbed per gram of 5-SA-TiO_2, the capacity decreased with increasing the amount of material. This may be attributed to the association of adsorption sites, resulting in a decrease in total surface area presented to the dye molecules and an increase in dispersion path length [35]. Meanwhile, from the Figure 5, it is observed that the photocatalytic degradation of MO increased from 51 % to 82.6 % with increasing the dosage of 5-SA-TiO_2 photoadsorbent from 0.02 to 0.08 g/L. It is due to the increase of active sites for the production of OH free radicals. However, the amount of dyes adsorbed and free dyes remains constant even with further addition of the 5-SA-TiO_2. Therefore, the optimum dosage of 5-SA-TiO_2 for the adsorption and photodegradation of MO was selected as 0.02 g/L in the experiments.

3.4. Effect of initial dye concentration on the adsorption and photocatalytic degradation of MO

The effect of initial dye concentration on the adsorption and photodegradiation of MO is shown in Figure 6. The adsorption of MO dye molecules decreased with an increase in the dye concentration. In other words, the amount of the MO adsorbed onto 5-SA-TiO_2 material increased with an increase in the initial dye concentration of solution if the amount of adsorbent was kept unchanged. This is due to the increase in the driving force of the concentration gradient with the higher initial dye concentration.

Therefore, the remaining amounts of dye molecules will be higher for high initial concentrations of dye. Furthermore, the effect of initial dye concentration on the degree of photocatalytic degradation using 5-SA-TiO_2 as catalyst was studied by varying initial dye concentrations from 5 to 20 mg/L. It is observed that the photocatalytic degradation of MO decreases with increasing the initial dye concentration.

The presumed reason is that, when the initial dye concentration is increased, more and more dye molecules are adsorbed on the surface of 5-SA-TiO_2. Therefore, the generation of OH free radicals will be reduced since the active sites for adsorption were covered by dye molecules. In addition, as the initial concentration of the MO increases, the photons get intercepted before they can reach the adsorbent surface. As a result, it has been found that the removal efficiency of MO is high for the photocatalytic degradation compared to that of adsorption process.

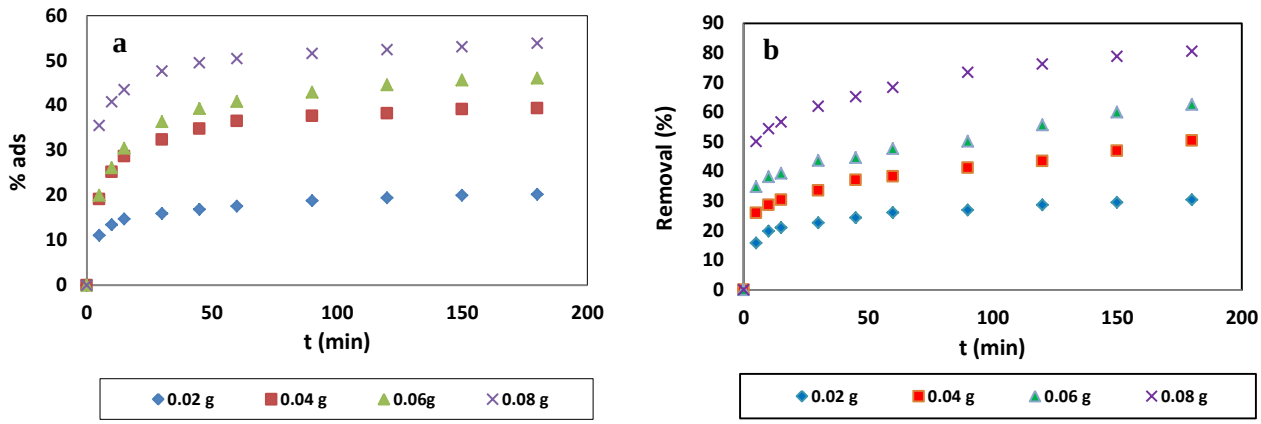

Figure 5: The effect of adsorbent dosage on the adsorption (a) and photodegradiation (b) of MO on 5-SA-TiO_2 (initial concentration 200 mg/L, pH = 5, T=298 K).

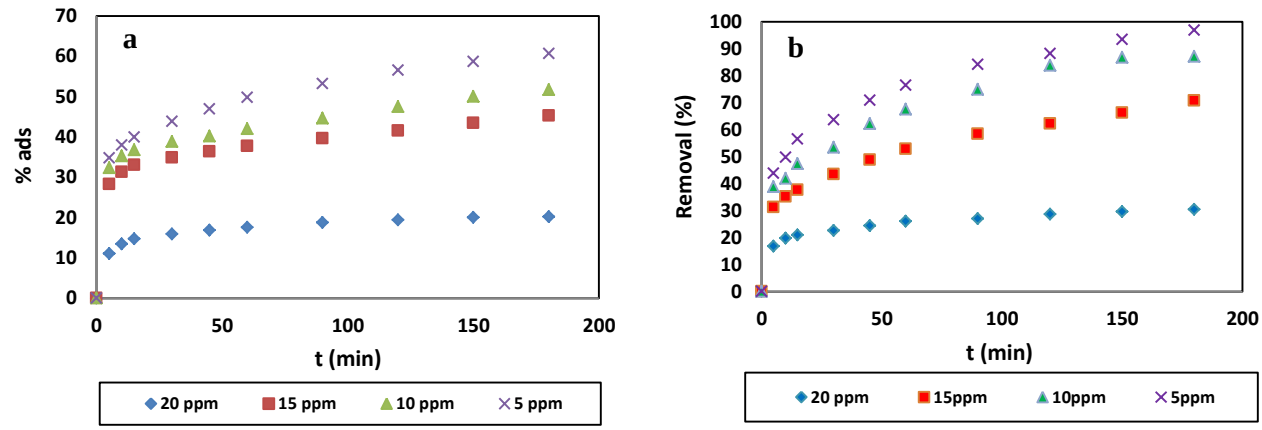

Figure 6: The effect of initial dye concentration on the the adsorption (a) and photodegradiation (b) of MO on 5-SA-TiO_2 (pH = 5, T=298 K and contact time 180 min).

3.5. Effect of temperature on the adsorption and photocatalytic degradation of MO

The effect of the temperature on MO removal from aqueose solutions by 5-SA-TiO_2 was studied at 298, 308 and 318 K, as shown in Figure 7. As the contact time was increased, similar increases in the MO removal efficiency were observed at different temperatures. The contact times required to removal efficiency of MO were approximately 50-60 min for the different temperatures. Moreover, the adsorption of MO decreased with increasing temperature as shown in Figure 7. Similar observations have been reported in the literature [36]. It can be explained by the fact that higher temperatures most certainly lead to an increase in the solubility of the MO organic dye. In addition, when temperature increased, the intermolecular forces between the organic compounds and the active sites of the adsorbent weakened. Therefore the MO dye was more difficult to adsorb.

3.6. Adsorption isotherm

It is important to evaluate the adsorption properties of 5-SA-TiO_2 adsorbent through analysis of the equilibrium data obtained from the experiments and the equilibrium relationship between adsorbed dye molecules and adsorbent. The adsorption equilibrium data collected from the MO dye concentrations (50-200 mg/L) and different temperatures were fitted by the Langmuir, the Freundlich and the Temkin isotherm models. The Langmuir isotherm theory assumes the monolayer coverage of adsorbate over a homogeneous adsorbent surface where all sorption sites are found to be identical and energetically equivalent, whereas the Frendlich isotherm model is valid for the multilayer adsorption on a heterogeneous adsorbent surface and predicts that the dye concentration on the adsorbent will increase with the increasing of the adsorbate concentration in the solution and lastly, the Temkin isotherm model assumes that the decrease in the heat of adsorption is linear and the adsorption is characterized by a uniform distribution of binding energies [37].

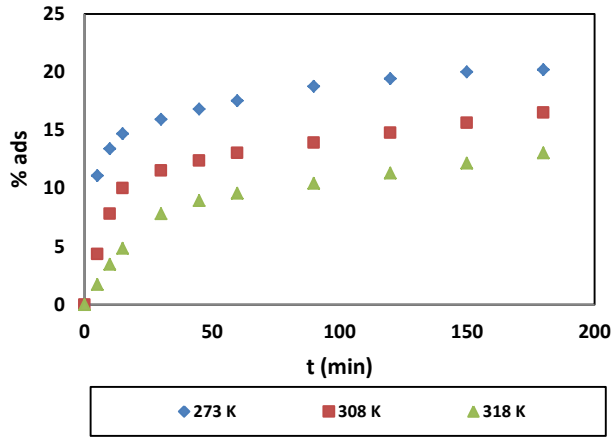

Figure 7: The effect of temperature on the adsorption of MO on 5-SA-TiO_2 nanoparticles (initial concentration 200 mg/L, pH = 5, and contact time 180 min).

The mathematical expression for the Langmuir isotherm is:

$$\frac{C_e}{q_e} = \left(\frac{1}{q_m\, b}\right) + \left(\frac{1}{q_m}\right) C_e \qquad (3)$$

where q_e (mg/g) is the amount of the dye adsorbed at the equilibrium, C_e (mg L^{-1}) is the equilibrium concentration of dye in solution, q_m (mg g^{-1}) is the Langmuir constant demonstrating maximum monolayer capacity, and b is the Langmuir constant associated with the sorption energy.

Freundlich isotherm can be expressed as follows:

$$q_e = K_f C_e^{1/n} \qquad (4)$$

where K_f((mg/g)$(Lmg^{-1})^{1/n}$) and n (dimensionless) are constants that account for all factors affecting the adsorption process, such as the adsorption capacity and intensity. The Freundlich constants K_f and 1/n can be respectively determined from the intercept and the slope of the linear plot of ln q_e versus ln C_e.

Temkin isotherm can be used in the following form:

$$q_e = A\, ln\, K_T + A\, ln\, C_e \qquad (5)$$

$$A = \frac{RT}{b} \qquad (6)$$

where K_T (mg/g) is the equilibrium binding constant corresponding to the maximum binding energy, the constant A and b are related to the heat of sorption and the heat of adsorption, respectively. Values of K_T and b were calculated from the intercept and slope of the plots of q_e versus ln C_e. The Langmuir, Freundlich and Temkin isotherm parameters and the correlation coefficient (R^2) are summarized in Table 1.

As illustrated in Table 1, the correlation coefficient (R^2) for the Temkin isotherm model was 0.999. In other words, the R^2 of the Temkin isotherm was greater than that of the two other isotherms for the adsorption of MO. This indicates that the adsorption of MO onto the 5-SA-TiO_2 nanoparticles adsorbent is better described by the Temkin isotherm model than the Langmuir and Freundlich isotherms.

In addition, the q_m value of MO on 5-SA-TiO_2 adsorbent have been compared with those of other adsorbents (Table 2). It was found that 5-sulfosalicylic acid-modified TiO_2 nanoparticles as adsorbent had a relatively high adsorption capacity (q_m) toward MO. Meanwhile, it has been found that the removal efficiency of MO is very high for the photocatalytic degradation compared to that of adsorption process.

Table 1: Langmuir, Freundlich and Temkin constants for adsorption of MO on 5-SA-TiO_2.

Langmuir			Freundlich			Temkin		
q_m (mg/g)	b (L/mg)	R^2	K_f ((mg/g))$(Lmg^{-1})^{1/n}$)	n	R^2	K_T	A	R^2
42.91	0.081	0.973	6.88	0.183	0.990	1.17	20.04	0.999

Table 2: The q_m values for the adsorption of MO on different adsorbents.

Adsorbent	Adsorption capacity (mg/g)	Reference
Chitosan	34.83	[38]
Protonated cross-linked chitosan	89.30	[39]
Y-Fe_2O_3/SiO_2/chitosan composite	34.29	[40]
Acid modified carbon coated monolith	147.06	[41]
Nanoporous core–shell Cu@Cu_2O nanocomposite	344.84	[42]
5-sulfosalicylic acid modified TiO_2	42.91	This work

Table 3: Kinetic constants of pseudo-first-order and pseudo-second-order models with correlation coefficients.

Removal process	Dye (mgg^{-1})	Pseudo-first-order			Pseudo-second-order		
		k_1 (min^{-1})	q_e (mgg^{-1})	R^2	k_2 (g $mg^{-1}min^{-1}$)	q_e (mgg^{-1})	R^2
Adsorption	5	0.016	167.3	0.99	0.0028	33.78	0.99
	10	0.015	181.2	0.92	0.0022	50	0.99
	15	0.013	221.4	0.97	0.0017	75.75	0.99
	20	0.014	69.3	0.98	0.0033	34.25	0.99
Photocatalytic degradation	5	0.0162	30.63	0.98	0.0183	4.5	0.99
	10	0.0178	48.62	0.98	0.0114	5.4	0.99
	15	0.0165	62.07	0.98	0.0094	44.6	0.99
	20	0.0191	19.10	0.99	0.0213	4.82	0.99

3.7. Decolorization kinetics

Several kinetic models were developed to understand both the photocatalytic degradation and adsorption kinetics. Kinetics study of photocatalytic decolorization of MO dye in the presence of 5-SA-TiO_2 particles was investigated at 5, 10, 15 and 20 mg/L, and the decolorization rate was monitored by studying the contact time up to 150 min. The mechanism of MO removal using the 5-SA-TiO_2 as photocatalyst was studied by the pseudo first-order and pseudo-second-order kinetic models. The liner plots of $ln(q_e-q_t)$ vs.t for the pseudo-first-order kinetic model and t/q_t vs. t for the pseudo-second-order kinetic model are shown in Figure 8 (photodegradation) and Figure 9 (adsorption). The constants of the two models with the correlation coefficients are shown in Table 3. As shown in Table 3, the value of the correlation coefficient R^2 for the pseudo-second-order model was greater than 0.99 for the photocatalytic degradeation process. The correlation coefficients of all initial MO concentrations are 0.99, which are very close to 1. These results show that the photocatalytic degradeation of MO dye in aqueous solutions using the 5-SA-TiO_2 particles can be described by pseudo-second-order kinetic model. A similar study was performed for MO adsorption onto 5-SA-TiO_2 as adsorbent (Table 3).

3.8. Thermodynamic studies

The temperature is usually an important factor which affects many adsorption processes, and it is an indicator of the adsorption nature. The termodynamic parameters, such as $\Delta H°$, $\Delta S°$ and $\Delta G°$ for 5-SA-TiO_2 can be related to the distribution coefficient of the solute between the solid and liquid phases. The effect of temperature on the adsorption and photocatalytic degradation of MO was evaluated at 298 K. The calculated thermodynamic parameters are given in Table 4. According to Table 4, the adsorption and photodegradation of MO using the 5-SA-TiO_2 are spontaneous.

Table 4. Thermodynamic parameters of the MO removal using the 5-SA-TiO_2 particles at 298 K.

Removal process	T (K)	C_e (mg L^{-1})	q_e (mg g^{-1})	K_c	$\Delta G°$ (kJ mol^{-1})	$\Delta H°$ (kJ mol^{-1})	$\Delta S°$ (J mol^{-1} K^{-1})
Adsorption	298	0.091	20.87	229.34	-13.428	-10.74	7.67
Photocatalytic degradation	298	0.80	43.75	546.87	-1.56	-	-

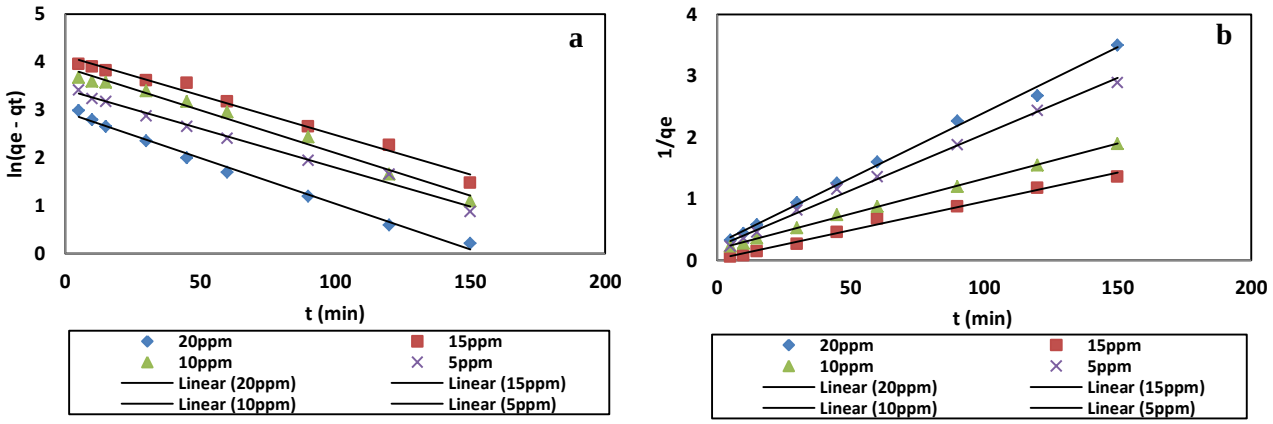

Figure 8: Pseudo-first-order (a) and pseudo-second-order (b) kinetic plots for photocatalytic process.

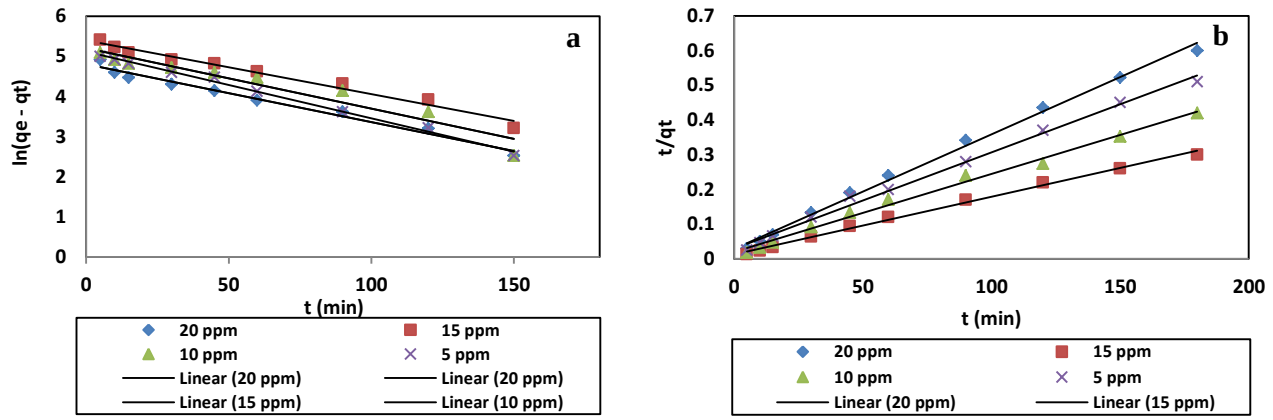

Figure 9: Pseudo-first-order (a) and pseudo-second-order (b) kinetic plots for adsorption process.

3.9. Proposed reaction mechanism

After surface modification of TiO_2 nanoparticles (self-assembly), both the adsorption ability and photodegradation activity were improved 2.26 and 5.13 times, respectively. The role of 5-sulfosalicylic acid on the improvements TiO_2 photocatalyst might be due to the enhancement of the affinity between MO and the 5-SA-TiO_2, larger surface areas by the reduction in particle size, and the increased formation of mobile OH radicals [43]. However, the photocatalytic reaction process can be proposed as follows [44].

$$TiO_2 + h\nu \rightarrow TiO_2\ (e^-, h^+) \quad (1)$$

$$h^+ + OH^- \rightarrow \cdot OH \quad (2)$$

$$e^- + O_2 \rightarrow O_2^- \quad (3)$$

MO + O_2^- or ·OH → peroxylated or hydroxylated intermediates → degraded products

3.10. Regeneration and reusability of 5-SA-TiO_2

The recovering and reusability of the 5-SA-TiO_2 photocatalyst was investigated for the removal of MO. In a typical experiment, 10 mL of an aqueous MO (20 mg/L) solution was mixed with 0.02 g of 5-SA-TiO_2 photocatalyst under UV light and stirred for 3 h in the optimum condition. The 5-SA-TiO_2 was subsequently collected from the solution by filtration and washed with ethanol. The washed 5-SA-TiO_2 photocatalyst was then used in the next experiment. This procedure was repeated for the eight absorption experiment cycle. The results show that the adsorption capacity of 5-SA-TiO_2 for MO was not significantly changed after four cycles which then slowly decreased. After six cycles, the MO removal efficiency was about 91.6%. Thus, results show the reusability of 5-SA-TiO_2 photocatalyst for MO removal.

4. Conclusion

Surface-modified titanium dioxide nanoparticles by 5-Sulfosalicylic acid (5-SA-TiO_2) were successfully synthesized and used for the adsorption and photodegradation of MO from aqueous solution. The structure analysis by SEM, XRD and FT-IR confirmed the surface modification of TiO_2 nanoparticles by 5-sulfosalicylic acid. The Temkin isotherm was found to be the best fitting isotherm model. Kinetic studies showed that both adsorption and photodegradation processes followed pseudo-second-order kinetics at a fixed adsorbent dosage. Thermodynamic studies showed that the adsorption process was spontaneous and exothermic. Comparison of photocatalytic activity and adsorption properties of 5-SA-TiO_2 clearly showed that the photocatalytic degradation process was more effective for decolorization of MO from the aqueous media.

5. References

1. Colour Index , Vol. 4, 3rd ed., The Society of Dyers and Colourists, Bradford, UK, 1971.
2. J. Griffiths, Photochemistry of azobenzene and its derivatives, A review., *Chem. Soc. Rev*., 1(1972), 481−493.
3. J. Y. Park, Y. Hirata, K. Hamada, Relationship between the dye/additive interaction and inkjetink droplet formation, *Dyes Pigm*., 95(2012), 502-511.
4. H. S. Freeman, A. T. Peters (Eds). Colorants for Non-Textile Applications, Elsevier, 2000.
5. D. H. Song, H. Y. Yoo, J. P. Kim, Synthesis of stilbene-based azo dyes and application for dichroic materials in poly(vinyl alcohol (polarizing films, *Dyes Pigm.*, 75(2007), 727-731.
6. D. M. Marmion, Handbook of US. Colorants, 3rd ed., John Wiley and Sons, Inc., New York, 1991.
7. G. Rosenfelder, J. Y. Chang, D. J. Braun ,Sphingosine determination at the picomole level using dimethylaminoazobenzene sulphonyl chloride, *J. Chromatogr. B: Biomed. Sci. App*., 272(1983), 21-27.
8. W. Huang, Y. Li, H. Lin, H. Lin, Colorimetric recognition of acetate anions in aqueous solution using charge neutral azo derivatives, *Spectrochim. Acta A*, 86(2012), 437-442.
9. N. Hosain Nataj, E. Mohajerani, H. Nemati, A. Moheghi, M.R. Yazdanbakhsh, M. Goli, A. Mohammadi, Studying optical and nonlinear optical properties of synthesized azo dyes doped in polymer and liquid crystal using birefringence and Z-scan techniques, *J. Appl. Polym. Sci*., 127(2013), 456-462.
10. F. Chami, M. R. Wilson, Molecular order in a chromonic liquid crystal: a molecular simulation study of the anionic azo dye sunset yellow, *J. Am. Chem. Soc.*, 132(2010), 7794-7802.
11. H. Métivier Pignon, C. Faur Brasquet, P. Le Cloirec, Adsorption of dyes onto activated carbon cloths: approach of adsorption mechanisms and coupling of ACC with ultrafiltration to treat coloured wastewaters, *Sep. Purif. Technol*., 31(2003), 3-11.
12. B. Zohra, K. Aicha, S. Fatima, B. Nourredine, D. Zoubir, Adsorption of Direct Red 2 on bentonite modified by cetyltrimethylammonium bromide, *Chem. Eng. J.* 136(2008), 295-305.
13. L. Zhou, C. Gao, W.J. Xu, Magnetic dendritic materials for highly efficient adsorption of dyes and drugs, *ACS Appl. Mater. Interfaces*, 5(2010), 1483-1491.
14. A. Khaled, A. E. Nemr, A. El Sikaily, O. Abdelwahab, Removal of Direct N Blue-106 from artificial textile dye effluent using activated carbon from orange peel:

Adsorption isotherm and kinetic studies, *J. Hazard. Mater*., 165(2009), 100-110.

15. D. S. Sun, X. D. Zhang, Y. D. Wu, X. Liu, Adsorption of anionic dyes from aqueous solution on fly ash, *J. Hazard. Mater.*, 181(2010), 335-342.
16. J. Basiri Parsa, S. Hagh Negahdar, Treatment of wastewater containing Acid Blue 92 dye by advanced ozone-based oxidation methods, *Sep. Purif. Technol.*, 98(2012), 315-320.
17. I. Khouni, B. Marrot, P. Moulin, R. Ben Amar, Decolourization of the reconstituted textile effluent by different process treatments: Enzymatic catalysis, coagulation/flocculation and nanofiltration processes, Desalination, 268(2011), 27-37.
18. J. H. Huang, C. F. Zhou, G. M. Zeng, X. Li, J. Niu, H. J. Huang, L. J. Shi, S. B. He, Micellar-enhanced ultrafiltration of methylene blue from dye wastewater via a polysulfone hollow fiber membrane, *J. Membr. Sci*., 365(2010), 138-144.
19. S. S. Madaeni, Z. Jamali, N. Islami, Highly efficient and selective transport of methylene blue through a bulk liquid membrane containing Cyanex 301 as carrier, *Sep. Purif. Technol*., 81(2011), 116-123.
20. P. Bradder, S. K. Ling, S. B. Wang, S. M. Liu, Dye Adsorption on Layered Graphite Oxide, *J. Chem. Eng. Data.*, 56(2010), 138-141.
21. A. Rodriguez, J. Garcia, G. Ovejero, M. Mestanza, Adsorption of anionic and cationic dyes on activated carbon from aqueous solutions: Equilibrium and kinetics, J. Hazard. Mater., 172(2009), 1311-1320.
22. G. Mc Kay, The adsorption of dyestuffs from aqueous solution using activated carbon: Analytical solution for batch adsorption based on external mass transfer, *Chem. Eng. J.*, 27(1983), 187-196.
23. R. Dolphen, N. Sakkayawong, R. Thiravetyan, W. Nakbanpote, Adsorption of Reactive Red 141 from wastewater onto modified chitin, *J. Hazard. Mater*., 145(2007), 250-255.
24. A. K. Chowdhury, A. D. Sarkar, A. Bandyopadhyay, Rice Husk Ash as a Low Cost Adsorbent for the Removal of Methylene Blue and Congo Red in Aqueous Phases, *Clean*, 37(2009), 581-591.
25. W. K. Backhaus, E. Klumpp, H. D. Narres, M. J. Schwuger, Adsorption of 2,4-Dichlorophenol on Montmorillonite and Silica: Influence of Nonionic Surfactants, *J. Colloid. Interf. Sci*., 242(2001), 6–13.
26. P. Mokhtari, M. Ghaedi, K. Dashtian, M. R. Rahimi, M. K. Purkait, Removal of methyl orange by copper sulfide nanoparticles loaded activated carbon: Kinetic and isotherm investigation, *J. Mol. Liq*., 219(2016), 299-305.
27. S. Jafari, F. Zhao, D. Zhao, M. Lahtinen, A. Bhatnagar, M. Sillanp, Modified nano-graphite/Fe3O4 composite as efficient adsorbent for the removal of methyl violet from aqueous solution, *J. Mol. Liq*., 196(2014), 348-356.
28. B. Kakavandi, R. Rezaei Kalantary, A. Esrafily, A. Jonidi Jafari, A. Azari, Isotherm, kinetic and thermodynamic of Reactive Blue 5 (RB5) dye adsorption using Fe_3O_4 nanoparticles and activated carbon magnetic composite, *J. Color. Sci. Tech.*, 7(2013), 238-247.
29. B. Tryba, A. W. Morawski, M. Inagaki, Application of TiO2-mounted activated carbon to the removal of phenol from water, *Appl. Cat. B.*, 41(2003), 427-433.
30. S. X. Li, F. Y. Zheng, W. L. Cai, A. Q. Han, Y. K. Xie, Surface modification of nanometer size TiO_2 with salicylic acid for photocatalytic degradation of 4-nitrophenol, *J. Hazard. Mater*., 135(2006), 431-436.
31. S. X. Li, F. Y. Zheng, X. L. Liu, F. Wu, N. S. Deng, J. H. Yang, Photocatalytic degradation of p-nitrophenol on nanometer size titanium dioxide surface modified with 5-sulfosalicylic acid, *Chemosphere*., 61(2005), 589-94.
32. S. X. Li, S. J. Cai, F. Y. Zheng, Self assembled TiO_2 with 5-sulfosalicylic acid for improvement its surface properties and photodegradation activity of dye, *Dyes Pigm*., 95(2012), 188-193.
33. S. J. Allen, G. Mc Kay, J. F. Porter, Adsorption isotherm models for basic dye adsorption by peat in single and binary component systems, *J. Colloid. Interface. Sci.*, 280(2004), 322-333.
34. H. Fallah Moafi, A. Fallah Shojaie, M. A. Zanjanchi, Titania and titania nanocomposites on cellulosic fibers: Synthesis, characterization and comparative study of photocatalytic activity, *Chem. Eng. J.*, 166(2011), 413–419.
35. X. S. Wang, Y. Zhou, Y. Yiang, C. Sun, The removal of basic dyes from aqueous solutions using agricultural by-products, *J. Hazard. Mater*., 157(2008), 374-385.
36. I. A. W. Tan, A. L. Ahmad, B. H. Hameed, Adsorption of basic dye on high-surface-area activated carbon prepared from coconut husk: Equilibrium, kinetic and thermodynamic studies, *J. Hazard. Mater*., 154(2008), 337-346.
37. G. Crini, P. M. Badot, Sorption Processes and Pollution: Conventional and Nonconventional

Sorbents, Presses Universitaires de Franche-Comté, Paris, France, 2010.
38. T. K. Saha, N. C. Bhoumik, S. Karmaker, M. G. Ahmed, H. Ichikawa, Y. Fukumori, dsorption of methyl orange onto chitosan from aqueous solution, J. *Water Resour. Prot*., 2 (2010) 898–906.
39. R. Huang, Q. Liu, J. Huo, B. Yang, Adsorption of methyl orange onto protonated cross-linked Chitosan, Arabian. *J. Chem.*, (2013), http://dx.doi.org/ 10.1016/ j. arabjc. 2013.05.017.
40. H. Y. Zhu, R. Jiang, Y. Q. Fu, J. H. Jiang, L. Xiao, Preparation, characterization and dye adsorption properties of γ-Fe_2O_3/SiO_2/chitosan composite, *Appl. Surf. Sci.*, 258(2011), 1337–1344.
41. Cheah, S. Hosseini, M. A. Khan, T. G. Chuah, T. S. Y. Choong, Acid modified carbon coated monolith for methyl orange adsorption, *Chem. Eng. J.*, 215–216(2013), 747–754.
42. T. Kou, Y. Wang, C. Zhang, J. Sun, Z. Zhang, Adsorption behavior of methyl orange onto nanoporous core–shell Cu@Cu_2O nanocomposite, *Chem. Eng. J.*, 223(2013), 76–83.
43. J. Kim, W. Choi, TiO_2 modified with both phosphate and platinum and its photocatalytic activities, *Appl. Catal. B.*, 106(2011), 39-42.
44. P. Tias, L.M. Penney, J.S. Timothy, Visible-light-mediated TiO_2 photocatalysis of fluoroquinolone antibacterial agents, *Environ. Sci. Technol.*, 41(2007), 4720–4727.

How to cite this article:
A. Mohammadi, A. Aliakbarzadeh Karimi, H. Fallah Moafi, Adsorption and Photocatalytic Properties of Surface-Modified TiO2 Nanoparticles for Methyl Orange removal from Aqueous Solutions, Prog. Color Colorants Coat., 9 (2016) 249-260.